Applied and Environmental Microbiology, July 2011, p. 4912–4923 Vol. 77, No. 14
0099-2240/11/$12.00 doi:10.1128/AEM.02527-10

Development of a *Streptomyces venezuelae*-Based Combinatorial Biosynthetic System for the Production of Glycosylated Derivatives of Doxorubicin and Its Biosynthetic Intermediates[▽]†

Ah Reum Han,[1] Je Won Park,[2,4] Mi Kyeong Lee,[3] Yeon Hee Ban,[2] Young Ji Yoo,[2] Eun Ji Kim,[2] Eunji Kim,[2] Byung-Gee Kim,[1] Jae Kyung Sohng,[4] and Yeo Joon Yoon[2]*

Interdisciplinary Programs of Bioengineering, Seoul National University, Seoul 151-742, Republic of Korea[1]; Department of Chemistry and Nano Sciences, Ewha Womans University, Seoul 120-750, Republic of Korea[2]; College of Pharmacy, Chungbuk National University, Cheongju 361-763, Republic of Korea[3]; and Department of Pharmaceutical Engineering, Institute of Biomolecule Reconstruction, Sun Moon University, Asan 336-708, Republic of Korea[4]

Received 26 October 2010/Accepted 11 May 2011

Doxorubicin, one of the most widely used anticancer drugs, is composed of a tetracyclic polyketide aglycone and L-daunosamine as a deoxysugar moiety, which acts as an important determinant of its biological activity. This is exemplified by the fewer side effects of semisynthetic epirubicin (4′-*epi*-doxorubicin). An efficient combinatorial biosynthetic system that can convert the exogenous aglycone ε-rhodomycinone into diverse glycosylated derivatives of doxorubicin or its biosynthetic intermediates, rhodomycin D and daunorubicin, was developed through the use of *Streptomyces venezuelae* mutants carrying plasmids that direct the biosynthesis of different nucleotide deoxysugars and their transfer onto aglycone, as well as the postglycosylation modifications. This system improved epirubicin production from ε-rhodomycinone by selecting a substrate flexible glycosyltransferase, AknS, which was able to transfer the unnatural sugar donors and a TDP-4-ketohexose reductase, AvrE, which efficiently supported the biosynthesis of TDP-4-*epi*-L-daunosamine. Furthermore, a range of doxorubicin analogs containing diverse deoxysugar moieties, seven of which are novel rhodomycin D derivatives, were generated. This provides new insights into the functions of deoxysugar biosynthetic enzymes and demonstrates the potential of the *S. venezuelae*-based combinatorial biosynthetic system as a simple biological tool for modifying structurally complex sugar moieties attached to anthracyclines as an alternative to chemical syntheses for improving anticancer agents.

Anthracyclines, effective anticancer drugs, have a basic 7,8,9,10-tetrahydro-5,12-naphthacenequinone structure that is glycosylated with one or more sugar residues. Doxorubicin and daunorubicin, produced by *Streptomyces peucetius*, are representative anthracyclines and are approved for clinical use in, for example, breast and small lung cancers, acute myeloid leukemia, and different sarcomas (1, 2). The anticancer activities of anthracyclines generally result from DNA damage via the inhibition of DNA topoisomerase II and the generation of free radicals, DNA binding and alkylation, and DNA intercalation (28). These activities are closely related to the sugar components, which usually participate in molecular recognition of cellular targets. Their presence and structure are therefore important, or even essential, to the biological activity of anthracyclines (45). The severe side effects of anthracycline, such as dose-dependent cardiotoxicity, have been the main problems associated with the therapeutic use of these drugs. The clinically important epirubicin (4′-*epi*-doxorubicin) has successfully overcome these side effects. It is a semisynthetic analogue of doxorubicin with an opposite configuration of the hydroxyl group at C-4 of the deoxysugar. It displays reduced cardiotoxicity while maintaining similar antitumor properties compared to doxorubicin (12). Therefore, alteration of the sugar portion of anthracyclines is hoped to produce the next generation of anticancer agents with improved activities and reduced toxicities. Great efforts have already been made over the last decade to modify the glycosylation patterns of natural products by combinatorial biosynthesis as an alternative to chemical modification of the structurally complex sugar moiety (31). 4′-*epi*-Daunorubicin had been produced directly by fermentation from an *S. peucetius* mutant in which the *dnmV* gene involved in the determination of the stereochemistry of the C-4′ hydroxyl group was replaced by *Streptomyces avermitilis avrE* or *Saccharopolyspora erythraea eryBIV*. However, the production level of epirubicin was too low to be quantified (24). Little progress to improve the biological production of epirubicin has been made. Consequently, it is still manufactured semisynthetically from doxorubicin aglycone or daunorubicin by several chemical steps. Moreover, combinatorial biosynthesis of the doxorubicin analogs containing diverse sugar moieties has not been reported.

The pikromycin-producing *Streptomyces venezuelae* ATCC 15439 has been developed as a favorable host for combinatorial biosynthesis and heterologous expression of natural product biosynthetic pathways originating in other organisms due to its fast growth and relative ease of genetic manipulation (10, 13–15, 33–35). In the present study, an *S. venezuelae*-based

* Corresponding author. Mailing address: Department of Chemistry and Nano Sciences, Ewha Womans University, Seoul 120-750, Republic of Korea. Phone: 82-2-3277-4082. Fax: 82-2-3277-3419. E-mail: joonyoon@ewha.ac.kr.

† Supplemental material for this article may be found at http://aem.asm.org/.

▽ Published ahead of print on 20 May 2011.

combinatorial biosynthetic system was constructed to convert exogenously fed doxorubicin aglycone ε-rhodomycinone (ε-RHO) into glycosylated doxorubicin analogs. This was achieved through the heterologous expression of different combinations of genes for the synthesis of various nucleotide-activated deoxysugars and their transfer to ε-RHO, as well as genes for further elaboration of rhodomycin D (a glycosylated form of ε-RHO) to doxorubicin in a mutant strain of doxorubicin-resistant *S. venezuelae* in which the entire pikromycin biosynthetic gene cluster was deleted (Fig. 1). This genetically amenable and fast-growing *S. venezuelae* system allowed the exploration of substrate flexibility of anthracycline glycosyltransferases to transfer desired sugars to aglycone as well as the ability of thymidine-5′-diphospho (TDP)-4-ketohexose reductases to synthesize TDP-4-*epi*-L-daunosamine to enhance the *in vivo* production of epirubicin from ε-RHO. Furthermore, 17 unnatural glycosylated derivatives of doxorubicin or its biosynthetic intermediates were generated (Fig. 2), demonstrating the potential of this *S. venezuelae* system for engineered generation of doxorubicin analogs with modified sugar moieties as well as other polyketides glycosylated with unnatural sugars (10, 13–15).

MATERIALS AND METHODS

Bacterial strains, culture conditions, and genetic manipulation. *Escherichia coli* DH5α was used for routine subcloning. *S. venezuelae* YJ028 lacking the pikromycin polyketide synthase genes and genes for the biosynthesis of TDP-D-desosamine (14) was used as a heterologous host and was maintained on SPA medium (1 g of yeast extract, 1 g of beef extract, 2 g of tryptose, 10 g of glucose, a trace amount of ferrous sulfate, and 15 g of agar/liter). Protoplast formation and transformation procedures of *S. venezuelae* were performed as described previously (16), and transformants of *S. venezuelae* were selected in R2YE agar plates (16) supplemented with appropriate antibiotics. The genomic DNAs were prepared from a variety of actinomycetes: *S. peucetius* ATCC 29050, *S. venezuelae* ATCC 15439, *S. venezuelae* ISP 5230, *Streptomyces avermitilis* K139, *Streptomyces galilaeus* ATCC 31615, *Streptomyces fradiae* ATCC 19609, *Streptomyces griseus* ATCC 10137, *Amycolaptosis orientalis* NRRL 18098, *Streptomyces antibioticus* ATCC 11891, *Streptomyces griseus* subsp. *griseus* NBRC 13350, and *Streptomyces nogalater* ATCC 27451. The sources of these strains were described in Table S1 in the supplemental material.

Construction of expression plasmids. The DNA fragments used for the construction of expression plasmids in the present study were amplified by PCR with the corresponding primers and template DNAs (see Table S1 in the supplemental material). PCR was performed by using *Pfu* polymerase (Fermentas) according to the manufacturer's recommended conditions. All PCR products were cloned into plasmid Litmus28 (New England Biolabs) and sequenced to confirm their authenticity. Doxorubicin resistance genes were cloned into the integrative plasmid pSET152 (4) derivative containing *ermE** promoter (40) and an apramycin resistance marker. To construct the plasmids expressing doxorubicin resistance genes, a BglII/HindIII fragment containing *drrA-drrB* and a HindIII/XbaI fragment containing *drrC* were PCR amplified from the genomic DNA of *S. peucetius* ATCC 29050, ligated into the BglII/XbaI sites of Litmus28, and moved into BamHI/XbaI sites of pSET152 downstream of the *ermE** promoter generating the plasmid pABC.

The genes involved in the conversion of ε-RHO to rhodomycin D or doxorubicin derivatives were cloned into the replicative plasmid pSE34 (49), *E. coli-Streptomyces* shuttle vector containing *ermE** promoter, and thiostrepton resistance marker. To construct plasmids harboring several genes, the following general method was used. The PacI/XbaI fragment containing one gene was cloned to PacI/SpeI-digested Litmus28 carrying other genes. This process was repeated until all of the genes involved in the conversion of ε-RHO to rhodomycin D (compound 1a), daunorubicin (compound 2a), doxorubicin (compound 3a), or their derivatives were combined in Litmus28 and then transferred into pSE34 digested with PacI/XbaI. Genes encoding glycosyltransferase/auxiliary protein pairs, TDP-4-ketohexose reductases, and other sugar biosynthetic enzyme sets were respectively substituted by using EcoRV/NdeI, SnaBI/AvrII, and ClaI/XbaI sites in Litmus28. The catalytic functions of the genes used in the present study are listed in Table 1. The constructed gene combinations are summarized in Table 2 (plasmids for the production of rhodomycin D, doxorubicin, 4′-*epi*-rhodomycin D, and epirubicin), and Table 3 (plasmids for the production of glycosylated derivatives of rhodomycin D and doxorubicin).

In order to generate pDNS1, the genes encoding the AknS/AknT glycosyltransferase/auxiliary protein pair and TDP-L-daunosamine biosynthetic enzymes were sequentially cloned in Litmus28 to produce pDNS1_lit28. The insert DNA of pDNS1_lit28 was digested with PacI/XbaI, and ligated to pSE34 to give pDNS1. To construct a pDNS1 derivative carrying *dnmQ-dnmS* instead of *aknT-aknS*, the EcoRV/NdeI fragment carrying *dnmQ-dnmS* was ligated into EcoRV/NdeI-digested pDNS1_lit28, generating pDNS2_lit28. The insert DNA of pDNS2_lit28 was cloned into pSE34 to produce pDNS2. Plasmids pDXR1 and pDXR2, containing postglycosylation modification genes were constructed by adding PacI/XbaI fragments released from pDNS1 into PacI/SpeI sites of pSE34 carrying *dnrK-dnrP-doxA* and *dnrK-dnrP-dnrV-doxA*, respectively. To generate plasmids expressing the genes encoding enzymes that convert ε-RHO to 4′-*epi*-rhodomycin D (compound 1b), SnaBI/AvrII fragment carrying *dnmV* in pDNS1_lit28 was replaced by the SnaBI/AvrII fragment containing *avrE*, producing pEDNS1_lit28. The PacI/XbaI fragment from pEDNS1_lit28 was ligated to pSE34, yielding pEDNS1. To construct pEDNS1 derivatives, in which *aknT-aknS* was replaced with the genes encoding other glycosyltransferase/auxiliary protein pairs, EcoRV/NdeI fragment carrying *dnmQ-dnmS*, *stfPII-stfG*, or *snogN-snogE* was ligated to pEDNS1_lit28 lacking *aknT-aknS*, and then the insert DNAs of pEDNS1_lit28 derivatives were independently cloned to pSE34 producing pEDNS2, pEDNS3, or pEDNS4, respectively. pEDNS1 derivatives carrying genes coding different TDP-4-ketohexose reductases were constructed by replacing *avrE* in pEDNS1 using SnaBI/AvrII sites with *grsB*, *evaE*, *jadV*, *oleU*, *tylCIV*, *strL*, or *snogC*, generating pEDNS5, pEDNS6, pRST1, pRST2, pRST3, pRST4, or pRST5, respectively. To construct several plasmids (pEVCS, pMDNS1, pMDNS2, pRDS, pMEDNS, pMRST, pDOLV, pDDGT, pLOLV, pLDGT, and pLRHM) that direct the biosynthesis of different deoxysugars and their attachment, ClaI/XbaI fragments carrying different sugar gene cassettes were separately cloned into ClaI/XbaI-digested pEDNS1_lit28. The PacI/XbaI fragments of the resulting plasmids were independently cloned into pSE34. The PacI/XbaI fragment released from pEDNS1, pRST1, pMDNS1, or pEVCS was cloned into the PacI/SpeI sites of pSE34 harboring *dnrK-dnrP-dnrV-doxA* to generate pEDXR, pRSDXR, pMDXR, or pEVDXR, respectively.

Production and analysis of anthracycline glycosides. *S. venezuelae* strains expressing different combinations of sugar biosynthetic genes, genes encoding glycosyltransferase/auxiliary protein pairs, and genes participating in postglycosylation modifications were cultivated at 30°C for 5 days on R2YE agar supplemented with 23.3 μM (10 mg/liter) ε-RHO. The extraction of the anthracyclines produced in the *S. venezuelae* cultures was carried out as follows. The grown culture was diced, extracted with 50% methanol, and then centrifuged at 5,000 × *g* for 10 min. The crude extract was passed through an Oasis HLB (Waters) solid-phase extraction column, preconditioned with 3 ml of methanol, followed by 3 ml of 50% (vol/vol) methanol. The column was washed with 3 ml of 50% (vol/vol) methanol and then air dried for ca. 30 s. The attached anthracyclines were eluted three times with 1 ml of 5% (vol/vol) methanolic formic acid, evaporated to dryness at room temperature by vacuum centrifugation. Rhodomycin D (compound 1a), daunorubicin (compound 2a), doxorubicin (compound 3a), and their glycosylated derivatives produced by *S. venezuelae* mutant strains were analyzed by high-performance liquid chromatography-electrospray ionization-tandem mass spectrometry (HPLC-ESI-MS/MS). Analytical HPLC-ESI-MS/MS was performed in a Waters/Micromass Quattro micro/MS interface using a Phenomenex Synergi Polar-RP column (150 mm by 4.6 mm, 4 μm) in positive-ion mode. The analytes were eluted at a flow rate of 250 μl/min using a gradient of 5 mM (wt/vol) ammonium acetate and 0.05% (vol/vol) acetic acid in water (solution A) and 80% (vol/vol) acetonitrile with the same additive concentrations (solution B) at 20 to 70% solution B for 25 min, increasing to 80% solution B for 15 min, maintained at 80% solution B for 9 min, and then reduced to 20% solution B for 11 min for column re-equilibration. Quantification was conducted in multiple-reaction-monitoring (MRM) mode using ESI-MS/MS by selecting the two mass ions set to detect a transition of the parent ion to the product ion specific to the selected analytes. The productivities of all of the anthracyclines produced in the *S. venezuelae*-based bioconversion system are summarized in Tables 2 and 3. Independent experiments were carried out in triplicate. Preparative HPLC was performed with the same analytical column and mobile phase as the analytical HPLC system for isolating and purifying rhodomycin D (compound 1a) and its derivatives. Samples were prepared for nuclear magnetic resonance (NMR) spectroscopy, by each compound being dissolved in 250 μl of CD_3OD and then placed in a 5-mm Shigemi advanced NMR microtube (Sigma) matched to the solvent. NMR data for each purified compound were

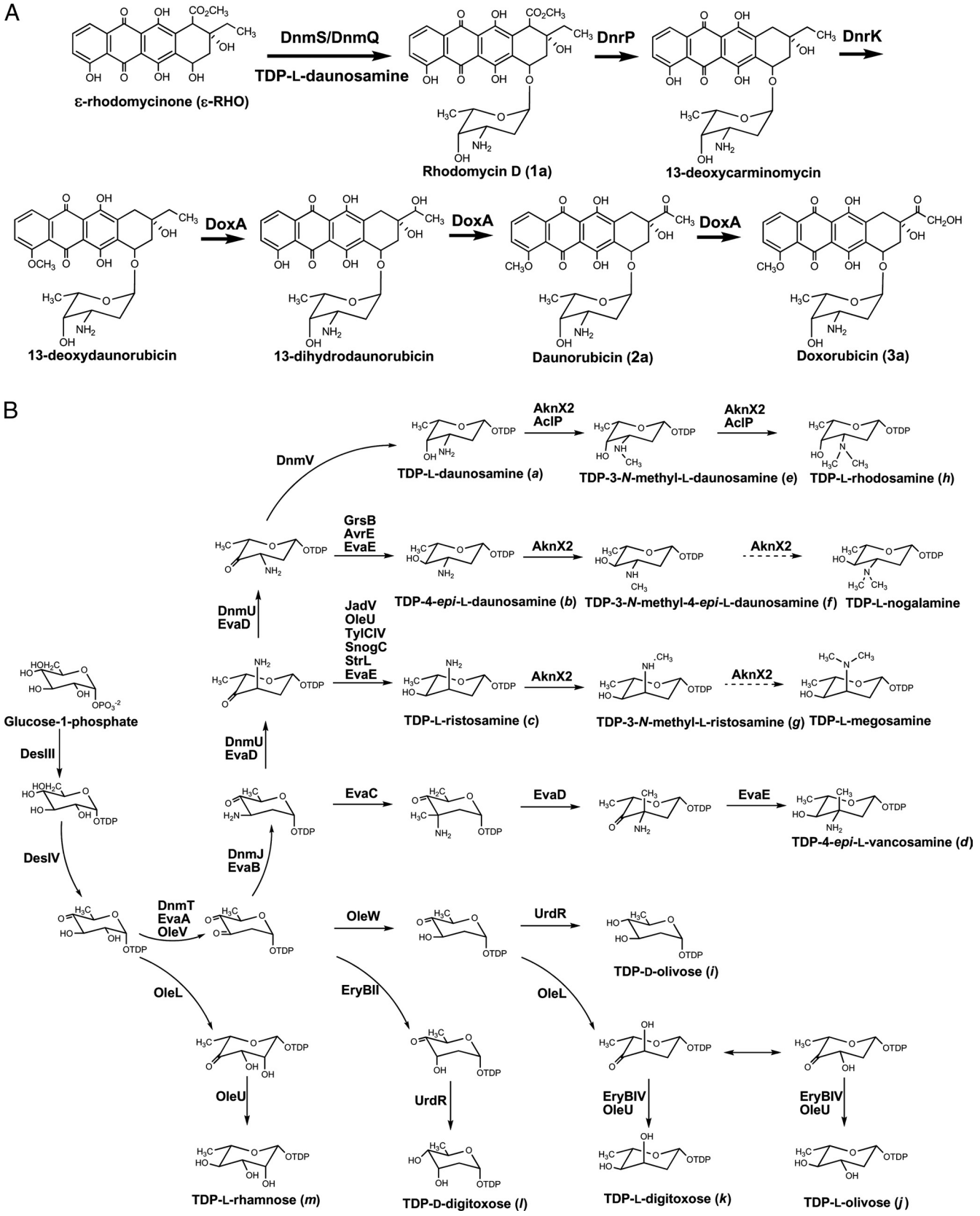

FIG. 1. Proposed pathways from ε-rhodomycinone into rhodomycin D, daunorubicin, and doxorubicin (A) and biosynthesis of the different deoxysugars directed by the plasmids described in the present study (B).

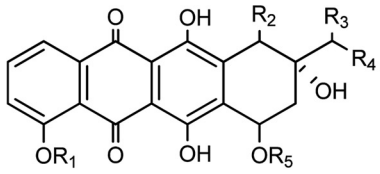

Compound	R_1	R_2	R_3	R_4	R_5
Rhodomycin D (1a)	H	CO_2CH_3	H	CH_3	a
4'-*epi*-rhodomycin D (1b)	H	CO_2CH_3	H	CH_3	b
L-ristosaminyl-rhodomycin D (1c)	H	CO_2CH_3	H	CH_3	c
4'-*epi*-L-vancosaminyl-rhodomycin D (1d)	H	CO_2CH_3	H	CH_3	d
3'-*N*-methyl-rhodomycin D (1e)	H	CO_2CH_3	H	CH_3	e
3'-*N*-methyl-4'-*epi*-rhodomycin D (1f)	H	CO_2CH_3	H	CH_3	f
3'-*N*-methyl-L-ristosaminyl-rhodomycin D (1g)	H	CO_2CH_3	H	CH_3	g
L-rhodosaminyl-rhodomycin D (1h)	H	CO_2CH_3	H	CH_3	h
D-olivosyl-rhodomycin D (1i)	H	CO_2CH_3	H	CH_3	i
L-olivosyl-rhodomycin D (1j)	H	CO_2CH_3	H	CH_3	j
L-digitoxosyl-rhodomycin D (1k)	H	CO_2CH_3	H	CH_3	k
D-digitoxosyl-rhodomycin D (1l)	H	CO_2CH_3	H	CH_3	l
L-rhamnosyl-rhodomycin D (1m)	H	CO_2CH_3	H	CH_3	m
Daunorubicin (2a)	CH_3	H	=O	CH_3	a
4'-*epi*-daunorubicin (2b)	CH_3	H	=O	CH_3	b
4'-*epi*-L-vancosaminyl-daunorubicin (2d)	CH_3	H	=O	CH_3	d
3'-*N*-methyl-daunorubicin (2e)	CH_3	H	=O	CH_3	e
Doxorubicin (3a)	CH_3	H	=O	CH_2OH	a
Epirubicin (3b)	CH_3	H	=O	CH_2OH	b
3'-*N*-methyl-doxorubicin (3e)	CH_3	H	=O	CH_2OH	e

FIG. 2. Proposed structures for rhodomycin D, daunorubicin, doxorubicin and their derivatives. Column R_5: a, L-daunosamine; b, 4-*epi*-L-daunosamine; c, L-ristosamine; d, 4-*epi*-L-vancosamine; e, 3-*N*-methyl-L-daunosamine; f, 3-*N*-methyl-4-*epi*-L-daunosamine; g, 3-*N*-methyl-L-ristosamine; h, L-rhodosamine; i, D-olivose; j, L-olivose; k, L-digitoxose; l, D-digitoxose; m, L-rhamnose.

acquired at 298 K on a Bruker Avance 500-MHz spectrometer. Proton and carbon chemical shifts were referenced to the tetramethylsilane signal. The structure of each compound was assigned based on its ^{1}H-NMR spectrum compared to literature values. ^{13}C analysis was also carried out if necessary. ε-RHO was purchased from Galilaeus (Kaarina, Finland). Standard doxorubicin (compound 3a), daunorubicin (compound 2a), and epirubicin (compound 3b) were obtained from GeneChem, Inc. (Daejeon, South Korea).

RESULTS

Construction of *S. venezuelae* mutant strains for bioconversion of ε-rhodomycinone to doxorubicin. To confer self-resistance to doxorubicin (compound 3a) in the anthracycline-nonproducing strain *S. venezuelae*, pABC carrying the three doxorubicin resistance genes *drrA*, *drrB* (9), and *drrC* (19) was introduced into the chromosome of *S. venezuelae* mutant YJ028 bearing a deletion of the entire pikromycin biosynthetic gene cluster encoding the polyketide synthases and TDP-D-desosamine biosynthetic enzymes, generating *S. venezuelae* YJ183. The mutant strain YJ183 was resistant to 25.9 μM commercially available doxorubicin hydrochloride, compared to a resistance to <1.7 μM in *S. venezuelae* YJ028. *S. venezuelae* YJ183 was used as heterologous host in subsequent experiments.

In order to biotransform ε-RHO to rhodomycin D (compound 1a), the first glycosylated intermediate of doxorubicin (compound 3a) biosynthesis in *S. peucetius* ATCC 29050 (Fig. 1A), two plasmids were constructed: pDNS1 and pDNS2, which contained sets of genes encoding the glycosyltransferase/auxiliary protein pair, together with TDP-L-daunosamine bio-

TABLE 1. Genes used in this study and their catalytic functions

Function[a]	Gene
NT	*desIII*
4,6-DH	*desIV*
2,3-DH	*evaA, dnmT, oleV*
3-AT	*evaB, dnmJ*
EP	*evaD, dnmU, oleL*
4-KR	*evaE, dnmV, avrE, jadV, urdR, grsB, tylCIV, oleU, strL, eryBV, snogC*
MT	*evaC*
N-MT	*aknX, aclP*
3-KR	*oleW, eryBII*
GT	*aknS/aknT, stfG/stfPII, snogE/snogN*
CDE	*dnrP*
COMT	*dnrK*
MO	*doxA*

[a] Abbreviations: NT, nucleotidyltransferase; 4,6-DH, 4,6-dehydratase; 2,3-DH, 2,3-dehydratase; 3-AT; 3-aminotransferase; EP, epimerase; 4-KR, 4-ketoreductase; MT, methyltransferase; N-MT, *N*-methyltransferase; 3-KR, 3-ketoreductase; GT, glycosyltransferase/auxiliary protein pair; CDE, 10-carbomethoxy-13-deoxycarminomycin esterase; COMT, carminomycin *o*-methyltransferase; MO, cytochrome P450 monooxygenase.

synthetic genes (29) (Table 2). For the biosynthesis of the common deoxysugar biosynthetic intermediate TDP-4-keto-6-deoxy-D-glucose, the glucose-1-phosphate thymidylyl transferase gene *desIII* and glucose-4,6-dehydratase gene *desIV* of *S. venezuelae* ATCC 15439 (48) were used instead of the corresponding genes in the TDP-L-danunosamine biosynthetic gene cluster of *S. peucetius* ATCC 29050. The AknS/AknT in pDNS1 encodes the rhodosaminyltransferase/auxiliary protein pair involved in the biosynthesis of aclacinomycin A from *S. galilaeus* ATCC 31615 (18), whereas pDNS2 contains *dnmS/dnmQ*, which encodes the glycosyltransferase/auxiliary protein pair participating in glycosylation of ε-RHO with TDP-L-daunosamine from *S. peucetius* ATCC 29050 (32). The auxiliary helper proteins such as AknT and DmnQ are required for efficient *in vivo* glycosylation (11, 21). Both pDNS1 and pDNS2 were independently introduced into *S. venezuelae* YJ183 to yield the mutant strains YJ183/pDNS1 and YJ183/pDNS2, respectively. The transformants were cultured on R2YE agar supplemented with ε-RHO, extracted by solid-phase extraction, and then analyzed by HPLC-ESI-MS/MS. The peak corresponding to rhodomycin D (compound 1a; 7-*O*-L-daunosaminyl-ε-RHO), selected at a mass transition from *m/z* 558 to 130, was detected by HPLC-ESI-MS/MS with a retention time (Rt) of 37.0 min (Fig. 3A and see Fig. S1-1B in the supplemental material for its MS/MS fragmentation pattern). The production of rhodomycin D (compound 1a) in YJ183/pDNS1 was 2.5-fold higher than in YJ183/pDNS2 (Table 2), indicating that *aknS/aknT* can more efficiently transfer TDP-L-daunosamine to the exogenous ε-RHO in the heterologous host *S. venezuelae.* Therefore, further study of modifications of rhodomycin D (compound 1a) to doxorubicin (compound 3a) was carried out using AknS as glycosyltransferase. Upon HPLC-ESI-MS/MS analysis, YJ183/pDXR1, carrying *dnrP*, *dnrK*, and *doxA*, which encode the enzymes responsible for the postglycosylation modifications of rhodomycin D (compound 1a) in the doxorubicin biosynthetic pathway (20, 22, 23), in addition to the genes contained in pDNS1, produced only

TABLE 2. Biosynthetic gene sets expressed in the engineered strain of *S. venezuelae* for bioconversion of ε-RHO to doxorubicin or epirubicin and productivities of doxorubicin, its intermediates, and epirubicin, by *S. venezuelae* mutant strains

Plasmid	Deoxysugar biosynthetic gene set	GT[a]	Post-GT[b]	Compound (productivity)[c]
DNS1	*desIII-desIV-dnmT-dnmJ-dnmU-dnmV*	*aknS/aknT*		1a (14.3 ± 0.21)
DNS2	*desIII-desIV-dnmT-dnmJ-dnmU-dnmV*	*dnmS/dnmQ*		1a (5.7 ± 0.65)
DXR1	*desIII-desIV-dnmT-dnmJ-dnmU-dnmV*	*aknS/aknT*	*dnrK-dnrP-doxA*	1a (10.8 ± 1.36)
DXR2	*desIII-desIV-dnmT-dnmJ-dnmU-dnmV*	*aknS/aknT*	*dnrK-dnrP-dnrV-doxA*	1a (2.8 ± 0.5) 2a (0.9 ± 0.04) 3a (1.1 ± 0.13)
EDNS1	*desIII-desIV-dnmT-dnmJ-dnmU-avrE*	*aknS/aknT*		1b (13.4 ± 2.51) 1c (0.2 ± 0.05)
EDNS2	*desIII-desIV-dnmT-dnmJ-dnmU-avrE*	*dnmS/dnmQ*		1b (0.1 ± 0.03)
EDNS3	*desIII-desIV-dnmT-dnmJ-dnmU-avrE*	*stfG/stfPII*		1b (10.9 ± 0.92)
EDNS4	*desIII-desIV-dnmT-dnmJ-dnmU-avrE*	*snogE/snogN*		1b (5.1 ± 1.16)
EDNS5	*desIII-desIV-dnmT-dnmJ-dnmU- grsB*	*aknS/aknT*		1b (0.2 ± 0.04)
EDNS6	*desIII-desIV-dnmT-dnmJ-dnmU- evaE*	*aknS/aknT*		1b (10.0 ± 1.02) 1c (4.8 ± 1.21)
RST1	*desIII-desIV-dnmT-dnmJ-dnmU-jadV*	*aknS/aknT*		1b (0.4 ± 0.06) 1c (15.2 ± 1.94)
RST2	*desIII-desIV-dnmT-dnmJ-dnmU-oleU*	*aknS/aknT*		1b (0.2 ± 0.06) 1c (15.1 ± 1.43)
RST3	*desIII-desIV-dnmT-dnmJ-dnmU-tylCIV*	*aknS/aknT*		1c (0.5 ± 0.14)
RST4	*desIII-desIV-dnmT-dnmJ-dnmU-strL*	*aknS/aknT*		1c (0.9 ± 0.07)
RST5	*desIII-desIV-dnmT-dnmJ-dnmU-snogC*	*aknS/aknT*		1c (0.7 ± 0.05)
EDXR	*desIII-desIV-dnmT-dnmJ-dnmU-avrE*	*aknS/aknT*	*dnrK-dnrP-dnrV-doxA*	1b (6.0 ± 1.22) 1c (0.38 ± 0.1) 2b (3.7 ± 0.23) 3b (0.9 ± 0.11)

[a] GT, glycosyltransferase/auxiliary protein-encoding gene pair.
[b] Post-GT, postglycosylation enzyme-encoding genes.
[c] Compounds: 1a, rhodomycin D; 2a, daunorubicin; 3a, doxorubicin; 1b, 4′-*epi*-rhodomycin D; 1c, L-ristosaminyl-rhodomycin D; 2b, 4′-*epi*-daunorubicin; 3b, epirubicin. The productivity is expressed as the mean concentration (μM) ± the standard error of the mean.

TABLE 3. Biosynthetic gene sets expressed in the engineered strain of *S. venezuelae* for bioconversion of ε-RHO to derivatives of rhodomycin D and doxorubicin and productivities of derivatives of rhodomycin D and doxorubicin by *S. venezuelae* mutant strains

Plasmid	Deoxysugar biosynthetic gene set	GT[a]	Post-GT[b]	Compound (productivity)[c]
EVCS	*desIII-desIV-evaA-evaB-evaD-evaE-evaC*	*aknS*/*aknT*		1b (0.04 ± 0.009) 1c (0.03 ± 0.004) 1d (1.0 ± 0.16)
MDNS1	*desIII-desIV-dnmT-dnmJ-dnmU-dnmV-aknX2*	*aknS*/*aknT*		1a (1.0 ± 0.07) 1e (14.9 ± 0.53) 1h (0.005 ± 0.002)
MDNS2	*desIII-desIV-dnmT-dnmJ-dnmU-dnmV-aclP*	*aknS*/*aknT*		1a (1.3 ± 0.05) 1e (10.5 ± 0.09) 1h (0.004 ± 0.0007)
RDS	*desIII-desIV-dnmT-dnmJ-dnmU-dnmV-aknX2-aclP*	*aknS*/*aknT*		1a (0.7 ± 0.04) 1e (14.0 ± 0.07) 1h (12.8 ± 0.51)
MEDNS	*desIII-desIV-dnmT-dnmJ-dnmU-avrE-aknX2*	*aknS*/*aknT*		1b (14.7 ± 1.78) 1f (0.7 ± 0.21)
MRST	*desIII-desIV-dnmT-dnmJ-dnmU-jadV-aknX2*	*aknS*/*aknT*		1b (0.2 ± 0.05) 1c (14.5 ± 2.15) 1g (0.8 ± 0.12)
DOLV	*desIII-desIV-oleV-urdR-oleW*	*aknS*/*aknT*		1i (0.3 ± 0.07)
LOLV	*desIII-desIV-oleV-oleL-oleU-oleW*	*aknS*/*aknT*		1j (0.6 ± 0.10) 1k (0.02 ± 0.005)
LDGT	*desIII-desIV-oleV-oleL-eryBIV-oleW*	*aknS*/*aknT*		1j (0.05 ± 0.009) 1k (0.3 ± 0.07)
DDGT	*desIII-desIV-oleV-urdR-eryBII*	*aknS*/*aknT*		1l (0.5 ± 0.05)
LRHAM	*desIII-desIV-oleL-oleU*	*aknS*/*aknT*		1m (0.3 ± 0.04)
RSDXR	*desIII-desIV-dnmT-dnmJ-dnmU-jadV*	*aknS*/*aknT*	*dnrK-dnrP-dnrV-doxA*	1c (12.5 ± 0.07)
EVDXR	*desIII-desIV-evaA-evaB-evaD-evaE-evaC*	*aknS*/*aknT*	*dnrK-dnrP-dnrV-doxA*	1d (0.7 ± 0.03) 2d (0.06 ± 0.0035)
MDXR	*desIII-desIV-dnmT-dnmJ-dnmU-dnmV-aknX2*	*aknS*/*aknT*	*dnrK-dnrP-dnrV-doxA*	1e (13.9 ± 1.86) 2e (0.1 ± 0.02) 3e (0.3 ± 0.02)

[a] GT, glycosyltransferase/auxiliary protein-encoding gene pair.
[b] Post-GT, postglycosylation enzyme-encoding genes.
[c] Compounds: 1a, rhodomycin D; 1b, 4′-*epi*-rhodomycin D; 1c, L-ristosaminyl-rhodomycin D; 1d, 4′-*epi*-L-vancosaminyl-rhodomycin D; 1e, 3′-*N*-methyl-rhodomycin D; 1f, 3′-*N*-methyl-4′-*epi*-L-daunosaminyl-rhodomycin D; 1g, 3′-*N*-methyl-L-ristosaminyl-rhodomycin D; 1h, L-rhodosaminyl-rhodomycin D; 1i, D-olivosyl-rhodomycin D; 1j, L-olivosyl-rhodomycin D; 1k, L-digitoxosyl-rhodomycin D; 1l, D-digitoxosyl-rhodomycin D; 1m, L-rhamnosyl-rhodomycin D; 2d, 4′-*epi*-L-vancosaminyl-daunorubicin; 2e, 3′-*N*-methyl-daunorubicin; 3e, 3′-*N*-methyl-doxorubicin. The productivity is expressed as the mean concentration (μM) ± the standard error of the mean.

rhodomycin D (compound 1a), whereas YJ183/pDXR2, which harbors the additional gene *dnrV*, produced rhodomycin D (compound 1a), daunorubicin (compound 2a; m/z 528 > 130 in MRM mode), and doxorubicin (compound 3a; m/z 544 > 130 in MRM mode) at Rts of 36.9, 30.5, and 26.0 min, respectively (Fig. 3B and Table 2; see also Fig. S1-2B and Fig. S1-3B in the supplemental material for the MS/MS fragmentation patterns of compounds 2a and 3a, respectively). These results are consistent with previous results implicating *dnrV* in enzymatic reactions catalyzed by DoxA, although its exact function was not established (20).

Bioconversion of ε-rhodomycinone to epirubicin. Epirubicin (compound 3b) production in the *S. venezuelae* system required the TDP-4-ketohexose reduction step which confers an equatorial C-4 hydroxyl group to TDP-4-keto-L-daunosamine, the glycosylation step attaching TDP-4-*epi*-L-daunosamine to ε-RHO, producing 4′-*epi*-rhodomycin D (compound 1b), and the postglycosylation steps leading to epirubicin (compound 3b). Glycosyltransferase/auxiliary protein pairs capable of converting ε-RHO to 4′-*epi*-rhodomycin D (compound 1b) efficiently were first screened using a TDP-4-*epi*-L-daunosamine biosynthetic gene cassette containing *avrE*, a gene encoding TDP-4-ketohexose reductase in the L-oleandrose biosynthetic pathway from *S. avermitilis* (46), in place of *dmnV* since it has already been reported that *avrE* can support 4′-*epi*-daunorubicin (compound 2b) production in *S. peucetius* (24). Four plasmids were constructed: pEDNS1, pEDNS2, pEDNS3, and pEDNS4 carrying *aknS*/*aknT*, *dnmS*/*dnmQ*, *stfG*/*stfPII*, and *snogE*/*snogN*, respectively (Table 2). StfG from *S. steffisburgensis* NRRL 3193 and SnogE from *S. nogalater* ATCC 27451 are glycosyltransferases involved in the biosynthesis of steffimycin and nogalamycin, respectively (30, 42). HPLC-ESI-MS/MS analyses showed that 4′-*epi*-rhodomycin D (compound 1b; 7-*O*-4′-*epi*-L-daunosaminyl-ε-RHO; m/z 558 > 130 in MRM mode) was detected at an Rt of 39.2 min from all of the YJ183 mutants carrying each of the constructed plasmids, with pEDNS1 supporting the highest production (Fig. 3C; see also Fig. S1-4B in the supplemental material for its MS/MS fragmentation pattern), confirming that AknS is the most efficient glycosyltransferase toward the unnatural sugar donor TDP-4-*epi*-L-daunosamine among the tested glycosyltransferases (Table 2). Interestingly, a new small peak with the same mass transition of the parent ion to the product ion and MS/MS fragmentation pattern as those of 4′-*epi*-rhodomycin D (compound 1b) was detected at an Rt of 45.2 min from the culture of YJ183/pEDNS1 and determined as a novel L-ristosaminyl-rhodomycin D (compound 1c; 7-*O*-L-ristosaminyl-ε-RHO) (Fig. 3C; see also Fig. S1-5B in the supplemental material for

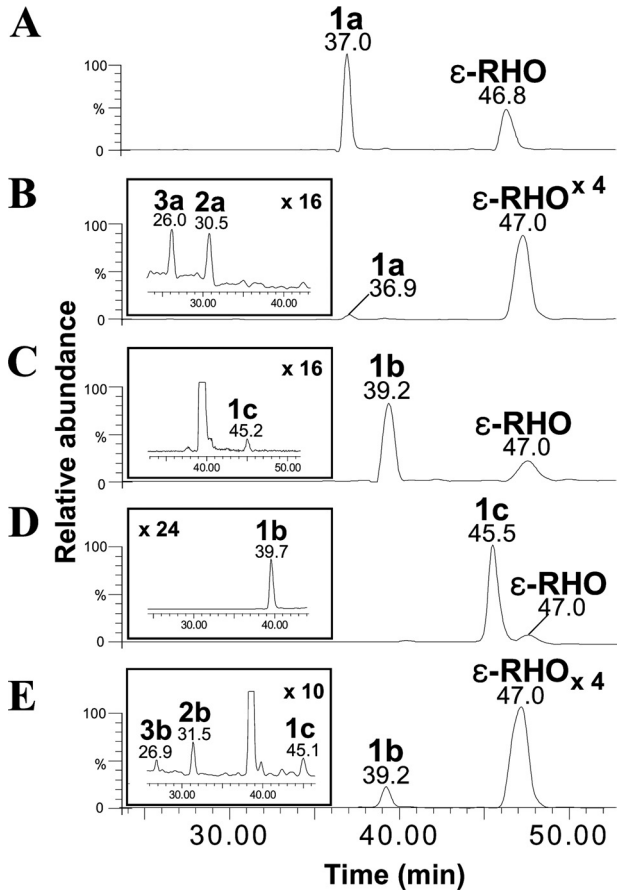

FIG. 3. HPLC-ESI-MS/MS chromatograms of cultures of S. *venezuelae* strains. (A) rhodomycin D (compound 1a; *m/z* 558 > 130) and ε-rhodomycinone (ε-RHO; *m/z* 429 > 322) detected from culture of YJ183/pDNS1. (B) Rhodomycin D (compound 1a; *m/z* 558 > 130) and ε-RHO (*m/z* 429 > 322) detected from culture of YJ183/pDXR2. The peaks of doxorubicin (compound 3a; *m/z* 544 > 130) and daunorubicin (compound 2a; *m/z* 528 > 130) are illustrated as an inset to chromatogram B. (C) 4′-*epi*-Rhodomycin D (compound 1b; *m/z* 558 > 130) and ε-RHO (*m/z* 429 > 322) detected from culture of YJ183/pEDNS1. The peak of L-ristosaminyl-rhodomycin D (compound 1c; *m/z* 558 > 130) is illustrated as an inset to chromatogram C. (D) L-Ristosaminyl-rhodomycin D (compound 1c; *m/z* 558 > 130) and ε-RHO (*m/z* 429 > 322) produced from culture of YJ183/pRST1. The 4′-*epi*-rhodomycin D (compound 1b; *m/z* 558 > 130) is illustrated as an inset to chromatogram D. (E) 4′-*epi*-Rhodomycin D (compound 1b; *m/z* 558 > 130) and ε-RHO (*m/z* 429 > 322) observed from culture of YJ183/pEDXR. The peaks of epirubicin (compound 3b; *m/z* 544 > 130), 4′-*epi*-daunorubicin (compound 2b; *m/z* 528 > 130), and L-ristosaminyl-rhodomycin D (1c; *m/z* 558 > 130) are illustrated as an inset to chromatogram E. The magnification factors of peak intensities of several compounds were displayed at the top of chromatograms.

its MS/MS fragmentation pattern), which might be generated by unexpected 5-epimerase activity of DmnU (Fig. 1B).

Next, several TDP-4-ketohexose reductases were tested for efficient biosynthesis of TDP-4-*epi*-L-daunosamine by constructing the pEDNS1 derivatives: pEDNS5, pEDNS6, pRST1, pRST2, pRST3, pRST4, and pRST5, which include *grsB* (GenBank accession no. AF128273; http://www.ncbi.nlm.nih.gov/GenBank/index.html), *evaE* (5), *jadV* (44), *oleU* (46), *tylCIV* (3), *strL* (37), and *snogC* (42), respectively, that encode TDP-4-ketohexose reductases in other deoxysugar biosynthetic pathways but act on different sugar intermediates (Table 2). Only small amounts of 4′-*epi*-rhodomycin D (compound 1b) were produced in the YJ183/pEDNS5 strain containing *grsB* (Table 2). Replacement of *avrE* by *evaE* (pEDNS6) led to the formation of twice as much 4′-*epi*-rhodomycin D (compound 1b) than L-ristosaminyl-rhodomycin D (compound 1c). *jadV* (pRST1; Fig. 3D) and *oleU* (pRST2) produced L-ristosaminyl-rhodomycin D (compound 1c) as major product and only trace amounts of 4′-*epi*-rhodomycin D (compound 1b) (Table 2). Strains YJ183/pRST3, YJ183/pRST4, and YJ183/pRST5 produced only small amounts of L-ristosaminyl-rhodomycin D (compound 1c), but no 4′-*epi*-rhodomycin D (compound 1b) (Table 2). No TDP-4-ketohexose reductase tested supported higher production of 4′-*epi*-rhodomycin D (compound 1b) than AvrE (Table 2). Based on the selection of AknS and AvrE as an efficient glycosyltransferase and 4-ketohexose reductase to support 4′-*epi*-rhodomycin D (compound 1b) production in a *S. venezuelae* system, pEDXR was constructed by adding a *dnrK-dnrP-dnrV-doxA* gene cassette into pEDNS1 to produce epirubicin (compound 3b) from ε-RHO (Table 2). HPLC-ESI-MS/MS analysis showed that YJ183/pEDXR produced epirubicin (compound 3b; 4′-*epi*-L-daunosaminyl-doxorubicinone; Rt, 26.9 min; *m/z* 544 > 130 in MRM mode), along with 4′-*epi*-rhodomycin D (compound 1b; Rt, 39.2 min), L-ristosaminyl-rhodomycin D (compound 1c; Rt, 45.1 min), and 4′-*epi*-daunorubicin (compound 2b; 4′-*epi*-L-daunosaminyl-daunorubicinone; Rt, 31.5 min; *m/z* 528 > 130 in MRM mode) (Fig. 3E and see Fig. S1-6B and Fig. S1-7B in the supplemental material for the MS/MS fragmentation patterns of compounds 2b and 3b, respectively).

Generation of glycosylated derivatives of rhodomycin D. The substrate flexibility of AknS for the unnatural sugar donor TDP-4-*epi*-L-daunosamine suggests the possibility of a combinatorial biosynthesis of unnatural rhodomycin D analogs containing diverse sugar moieties. The plasmids pEVCS, pDOLV, pDDGT, pLOLV, pLDGT, and pLRHM containing combinations of genes for the biosynthesis of TDP-4-*epi*-L-vancosamine (5), TDP-D-olivose (39), TDP-D-digitoxose (36), TDP-L-olivose (8), TDP-L-digitoxose (8), and TDP-L-rhamnose (39) (Table 3), respectively, as well as *aknS*/*aknT*, were constructed based on previous studies. In addition, three further plasmids were constructed: pMDNS1, pMEDNS, and pMRST, which contained the newly designed biosynthetic pathways directing the biosynthesis of TDP-L-rhodosamine (38), TDP-L-nogalamine (42), and TDP-L-megosamine (43), respectively.

YJ183/pEVCS produced 4′-*epi*-L-vancosaminyl-rhodomycin D (compound 1d; 7-*O*-4′-*epi*-L-vancosaminyl-ε-RHO; Rt, 40.7 min; *m/z* 572 > 144 in MRM mode) as expected, 4′-*epi*-rhodomycin D (compound 1b; Rt, 39.7 min), and L-ristosaminyl-rhodomycin D (compound 1c; Rt, 45.7 min), probably due to the skipping of the C-3 methylation step catalyzed by EvaC (Fig. 4A and Table 3; see also Fig. S1-8B in the supplemental material for the MS/MS fragmentation pattern of compound 1d). YJ183/pMDNS1 produced 3′-*N*-methyl-rhodomycin D (compound 1e; 7-*O*-3′-*N*-methyl-L-daunosaminyl-ε-RHO; Rt, 39.1 min; *m/z* 572 > 144 in MRM mode), an *N*-monomethylated biosynthetic intermediate of L-rhodosaminyl-rhodomycin D, as a major product and its biosynthetic intermediate rhodomycin D (compound 1a) (Fig. 4B and Table 3; see also Fig. S1-9B in the supplemental material for the MS/MS fragmen-

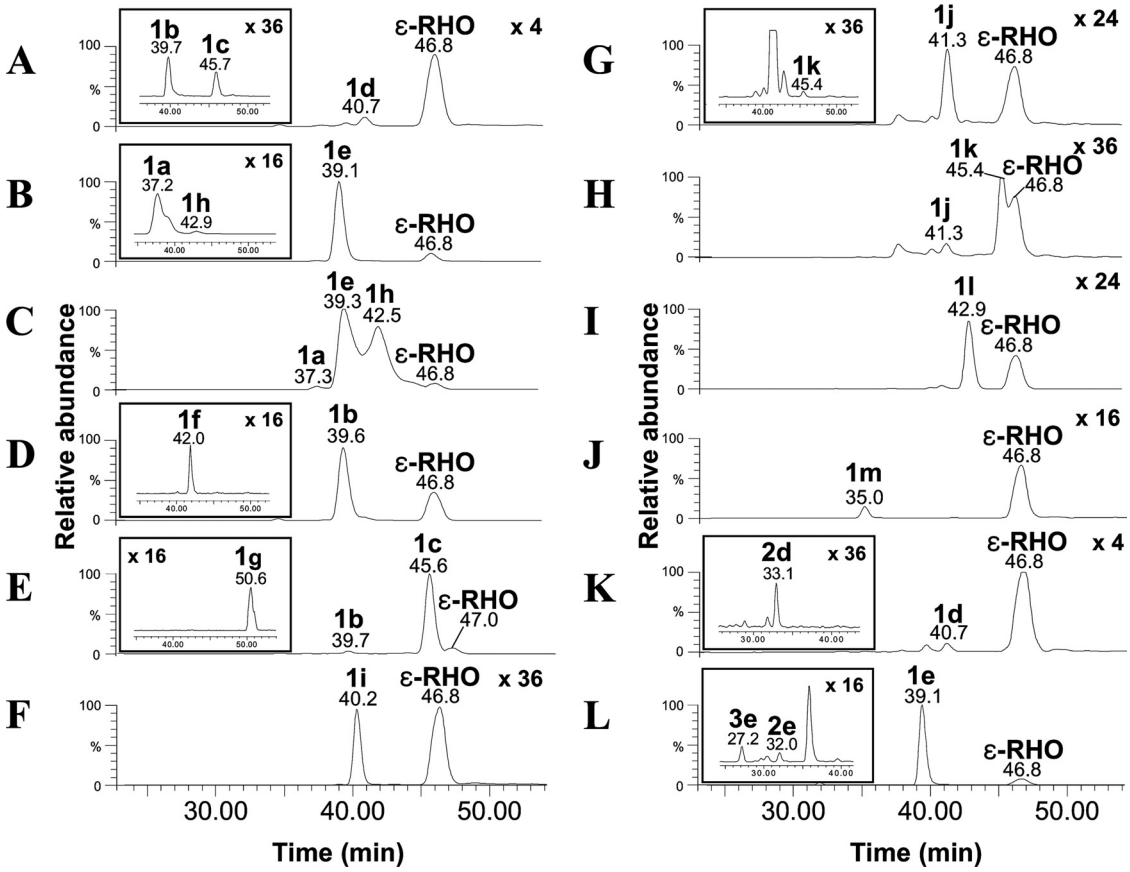

FIG. 4. HPLC-ESI-MS/MS chromatograms of cultures of *S. venezuelae* strains. (A) 4′-*epi*-L-Vancosaminyl-rhodomycin D (compound 1d; *m/z* 572 > 144) and ε-RHO (*m/z* 429 > 322) detected from culture of YJ183/pEVCS. The peaks of 4′-*epi*-rhodomycin D (compound 1b; *m/z* 558 > 130) and l-ristosaminyl-rhodomycin D (compound 1c; *m/z* 558 > 130) are illustrated as an inset to chromatogram A. (B) 3′-*N*-Methyl-rhodomycin D (compound 1e; *m/z* 572 > 144) and ε-RHO (*m/z* 429 > 322) detected from culture of YJ183/pMDNS1. The peaks of rhodomycin D (compound 1a; 558 > 130) and L-rhodosaminyl-rhodomycin D (compound 1h; *m/z* 586 > 158) are illustrated as an inset to chromatogram B. (C) Rhodomycin D (compound 1a; *m/z* 558 > 130), 3′-*N*-methyl-rhodomycin D (compound 1e; *m/z* 572 > 144), and L-rhodosaminyl-rhodomycin D (compound 1h; *m/z* 586 > 158) detected from culture of YJ183/pRDS. (D) 4′-*epi*-Rhodomycin D (compound 1b; *m/z* 558 > 130) and ε-RHO (*m/z* 429 > 322) detected from culture of YJ183/pMEDNS. The peak of 3′-*N*-methyl-4′-*epi*-rhodomycin D (compound 1f; *m/z* 572 > 144) is illustrated as an inset to chromatogram D. (E) 4′-*epi*-Rhodomycin D (1b; *m/z* 558 > 130) and L-ristosaminyl-rhodomycin D (compound 1c; *m/z* 558 > 130) detected from culture of YJ183/pMRST. The peak of 3′-*N*-methyl-L-ristosaminyl-rhodomycin D (compound 1g; *m/z* 572 > 144) is illustrated as an inset to chromatogram E. (F) D-Olivosyl-rhodomycin D (compound 1i; *m/z* 559 > 393) and ε-RHO (*m/z* 429 > 322) observed from culture of YJ183/pDOLV. (G) L-Olivosyl-rhodomycin D (compound 1j; *m/z* 559 > 393) and ε-RHO (*m/z* 429 > 322) observed from culture of YJ183/pLOLV. The peak of L-digitoxosyl-rhodomycin D (compound 1k; *m/z* 559 > 393) is illustrated as an inset to chromatogram G. (H) L-Olivosyl-rhodomycin D (compound 1j; *m/z* 559 > 393), L-digitoxosyl-rhodomycin D (compound 1k; *m/z* 559 > 393), and ε-RHO (*m/z* 429 > 322) observed from culture of YJ183/pLDGT. (I) D-Digitoxosyl-rhodomycin D (compound 1l; *m/z* 559 > 393) and ε-RHO (*m/z* 429 > 322) observed from culture of YJ183/pDDGT. (J) L-Rhamnosyl-rhodomycin D (compound 1m; *m/z* 575 > 393) and ε-RHO (*m/z* 429 > 322) observed from culture of YJ183/pLRHM. (K) 4′-*epi*-L-Vancosaminyl-rhodomycin D (compound 1d; 572 > 144) and ε-RHO (*m/z* 429 > 322) observed from culture of YJ183/pEVDXR. The peak of 4′-*epi*-L-vancosaminyl-daunorubicin (compound 2d; *m/z* 542 > 144) is illustrated as an inset to chromatogram K. (L) 3′-*N*-Methyl-rhodomycin D (compound 1e; 572 > 144) and ε-RHO (*m/z* 429 > 322) observed from culture of YJ183/pMDXR. The peaks of 3′-*N*-methyl-doxorubicin (compound 3e; *m/z* 558 > 144) and 3′-*N*-methyl-daunorubicin (compound 2e; *m/z* 542 > 144) are illustrated as an inset to chromatogram L. The magnification factors of peak intensities of several compounds were displayed at the top of chromatograms.

tation pattern of compound 1e). A small peak attributable to L-rhodosaminyl-rhodomycin D (compound 1h; 7-*O*-L-rhodosaminyl-ε-RHO; Rt, 42.9 min; *m/z* 586 > 158 in MRM mode) was also detected from YJ183/pMDNS1 (Fig. 4B and Table 3; see also Fig. S1-10B in the supplemental material for the MS/MS fragmentation pattern of compound 1h). pMDNS2 was constructed in which the *N*-methyltransferase gene *aknX2* of the aclacinomycin A-producing *S. galilaeus* ATCC 31615 was replaced with *aclP* from another aclacinomycin A producer, *S. galilaeus* ATCC 31133 (Table 3). YJ183/pMDNS2 showed a similar production pattern to YJ183/pMDNS1 (Table 3). However, YJ183/pRDS, containing both *aknX2* and *aclP*, produced significant amounts of a compound predicted to be L-rhodosaminyl-rhodomycin D (compound 1h) (Fig. 4C and Table 3). YJ183/pMEDNS produced a compound predicted to be 3′-*N*-methyl-4′-*epi*-rhodomycin D (compound 1f; 7-*O*-3′-*N*-methyl-4′-*epi*-L-daunosaminyl-ε-RHO; Rt, 42.0 min; *m/z* 572 > 144 in MRM mode) and its biosynthetic intermediate 4′-*epi*-rhodomycin D (compound 1b), but no -L-nogalosaminyl-rhodomycin D (Fig. 4D and Table 3; see also Fig.

S1-11B in the supplemental material for the MS/MS fragmentation pattern of compound 1f), suggesting that the *N*-methyltransferase AknX2 acted as a monomethyltransferase on TDP-4′-*epi*-L-daunosamine. YJ183/pMRST also generated a compound consistent with the mass of monomethylated L-ristosaminyl-rhodomycin D (compound 1g; 7-*O*-3′-*N*-methyl-L-ristosaminyl-ε-RHO; Rt, 50.6 min; *m/z* 572 > 144 in MRM mode), its biosynthetic intermediate L-ristosaminyl-rhodomycin D (compound 1c), and a trace amount of 4′-*epi*-rhodomycin D (compound 1b), but no L-megosaminyl-rhodomycin D (Fig. 4E and Table 3; see also Fig. S1-12B in the supplemental material for the MS/MS fragmentation pattern of compound 1g). This result again indicates that AknX2 functioned as a monomethyltransferase toward TDP-L-ristosamine. As anticipated, HPLC-ESI-MS/MS analysis of the culture extract of YJ183/pDOLV produced a peak consistent with the mass of D-olivosyl-rhodomycin D (compound 1i; 7-*O*-D-olivosyl-ε-RHO; Rt, 40.2 min; *m/z* 559 > 393 in MRM mode) (Fig. 4F and Table 3; see also Fig. S1-13B in the supplemental material for the MS/MS fragmentation pattern of compound 1i). YJ183/pLOLV and YJ183/pLDGT, respectively, produced compounds consistent with the mass of L-olivosyl-rhodomycin D (compound 1j; 7-*O*-L-olivosyl-ε-RHO; Rt, 41.3 min; *m/z* 559 > 393 in MRM mode) and L-digitoxosyl-rhodomycin D (compound 1k; 7-*O*-L-digitoxosyl-ε-RHO; Rt, 45.4 min; *m/z* 559 > 393 in MRM mode) as major products (Fig. 4G and H and Table 3; see also Fig. S1-14B and Fig. S1-15B in the supplemental material for the MS/MS fragmentation patterns of compounds 1j and 1k, respectively), with small amounts of the other compound, probably due to tautomerization between TDP-4-keto-L-olivose and TDP-4-keto-L-digitoxose (8). Peaks consistent with the masses of D-digitoxosyl-rhodomycin D (compound 1l; 7-*O*-D-digitoxosyl-ε-RHO; Rt, 42.9 min; *m/z* 559 > 393 in MRM mode) and L-rhamnosyl-rhodomycin D (compound 1m; 7-*O*-L-rhamnosyl-ε-RHO; Rt, 35.0 min; *m/z* 575 > 393 in MRM mode) were observed in the culture extracts of YJ183/pDDGT and YJ183/pLRHM, respectively (Fig. 4I and J and Table 3; see also Fig. S1-16B and Fig. S1-17B in the supplemental material for the MS/MS fragmentation patterns of compounds 1l and 1m, respectively).

Generation of glycosylated derivatives of doxorubicin. In order to modify further the relatively abundant glycosylated rhodomycin D derivatives 4′-*epi*-L-vancosaminyl-rhodomycin D (compound 1d), 3′-*N*-methyl-rhodomycin D (compound 1e), and L-ristosaminyl-rhodomycin D (compound 1c) into their glycosylated analogs of doxorubicin, the plasmids pEVDXR, pMDXR, and pRSDXR were constructed by adding the four genes *dnrP*, *dnrK*, *doxA*, and *dnrV* into pEVCS, pMDNS1, and pRST1, respectively. When pEVDXR was expressed in *S. venezuelae* mutant YJ183, metabolites expected to 4′-*epi*-L-vancosaminyl-daunorubicin (compound 2d; 7-*O*-4′-*epi*-L-vancosaminyl-daunorubicinone; Rt, 33.1 min; *m/z* 542 > 144 in MRM mode) and 4′-*epi*-L-vancosaminyl-rhodomycin D (compound 1d) were produced (Fig. 4K and Table 3; see also Fig. S1-18B in the supplemental material for the MS/MS fragmentation pattern of compound 1d). From the organic extract of YJ183/pMDXR supplemented with ε-RHO, three peaks were observed at Rts of 27.2, 32.0, and 39.1 min, predicted to be 3′-*N*-methyl-doxorubicin (compound 3e; 7-*O*-3′-*N*-methyl-L-daunosaminyl-doxorubicinone; *m/z* 558 > 144 in MRM mode), 3′-*N*-methyl-daunorubicin (compound 2e; 7-*O*-3′-*N*-methyl-L-daunosaminyl-daunorubicinone; *m/z* 542 > 144 in MRM mode), and 3′-*N*-methyl-rhodomycin D (compound 1e), respectively (Fig. 4L and Table 3; see also Fig. S1-19B and S1-20B in the supplemental material for the MS/MS fragmentation patterns of compounds 2e and 3e, respectively). YJ183/pRSDXR led to the production of only L-ristosaminyl-rhodomycin D (compound 1c) but not any glycosylated derivatives of doxorubicin and daunorubicin (data not shown).

Structural elucidation of glycosylated derivatives of rhodomycin D. The structures of the anthracycline derivatives generated in small amounts from *S. venezuelae* YJ183 mutant strains were predicted based on the ESI-MS/MS fragmentation patterns of the glycosylated anthracyclines (see Fig. S1 in the supplemental material). Although the configurations of sugar moieties cannot be determined by ESI-MS/MS, they were predicted from the deduced catalytic specificities of the sugar biosynthetic enzymes. However, the structures of rhodomycin D (compound 1a), 4′-*epi*-rhodomycin D (compound 1b), L-ristosaminyl-rhodomycin D (compound 1c), 4′-*epi*-L-vancosaminyl-rhodomycin D (compound 1d), and 3′-*N*-methyl-rhodomycin D (compound 1e) were deduced mainly by the chemical shifts of particular protons in NMR (see the supplemental material). The limited amounts of purified rhodomycin D and its derivatives did not allow the precise determination of coupling constants from 2D NMR.

The structure of rhodomycin D (compound 1a) was deduced from the spectroscopic data by comparison with literature values (6, 17; see also the supplemental material). The ^{1}H-NMR chemical shifts of 4′-*epi*-rhodomycin D (compound 1b) were similar to those of rhodomycin D (compound 1a) except for the upfield shifts of H-4′ and H-5′, suggesting the presence of 4′-*epi*-L-daunosamine as a sugar moiety (7; see also the supplemental material). The ESI-MS/MS spectrum of L-ristosaminyl-rhodomycin D (compound 1c) was similar to those of rhodomycin D (compound 1a) and 4′-*epi*-rhodomycin D (compound 1b) (see the supplemental material). The ^{1}H-NMR data of L-ristosaminyl-rhodomycin D (compound 1c) were also largely similar to those of rhodomycin D (compound 1a) except for the upfield shifts of H-3′ and H-4′ (see the supplemental material). In addition, characteristic signals for the L-ristosaminyl moiety were observed at δ_C49.27 (C-3′), δ_C71.18 (C-4′), and δ_C64.07 (C-5′) in the ^{13}C-NMR spectrum (26; see also the supplemental material). Therefore, the structure of L-ristosaminyl-rhodomycin D (compound 1c), which has not been reported yet, could be deduced from the ^{1}H- and ^{13}C-NMR data. The ^{1}H-NMR chemical shifts of 4′-*epi*-L-vancosaminyl-rhodomycin D (compound 1d) were similar to those of 4′-*epi*-rhodomycin D (compound 1b) (see the supplemental material). However, an additional methyl signal at δ_H1.45 (3′-CH_3) was shown instead of the H-3′ signal from 4′-*epi*-rhodomycin D (compound 1b), which is characteristic of the 4′-*epi*-L-vancosamine moiety (26, 41). The ^{1}H-NMR data of 3′-*N*-methyl-rhodomycin D (compound 1e) was similar to that of rhodomycin D, but for differences in the sugar moiety signals (see supplementary text). In the ^{13}C-NMR data, additional methyl signals appeared at δ_C30.45, suggesting the presence of a 7′-CH_3 moiety (see the supplemental material). The structure of 3′-*N*-methyl-rhodomycin D (compound 1e), which

has not yet been reported, was predicted by the ^{1}H- and ^{13}C-NMR data.

DISCUSSION

The simple *S. venezuelae*-based combinatorial biosynthetic system developed here facilitated improved biological production of epirubicin by selecting an efficient TDP-4-ketohexose reductase, AvrE, and glycosyltransferase, AknS, which were able to synthesize and transfer unnatural TDP-4-*epi*-L-daunosamine to ε-RHO. Although an *S. peucetius* mutant in which *dnmV* was substituted with *avrE* has been reported to produce 4′-*epi*-daunorubicin with trace amounts of epirubicin, the present study is, to the best of our knowledge, the first report of a considerable amount of epirubicin (0.9 μM ≈ 0.5 mg/liter) being produced by a biological method. The accumulation of large amounts of 4′-*epi*-rhodomycin D (compound 1b) in the YJ183/pEDXR strain (Fig. 3E) and the low conversion yields of rhodomycin D derivatives into doxorubicin derivatives in YJ183 strains expressing pEVDXR, pMDXR, and pRSDXR (Fig. 4K and L and Table 3) suggest that the postglycosylation modification steps catalyzed by DnrP, DnrK, and DoxA are rate-limiting and that engineering of more efficient postglycosylational modification enzymes could further enhance epirubicin production. Furthermore, two doxorubicin derivatives (compounds 3b and 3e), three daunorubicin derivatives (compounds 2b, 2d, and 2e), and 12 rhodomycin D derivatives (compounds 1b to 1m) were generated, as well as doxorubicin (compound 3a) and its intermediates (compounds 1a and 2a). Among the 20 anthracyclines produced in the present study, seven glycosylated derivatives of rhodomycin D (compounds 1c, 1e to 1g, 1i, 1k, and 1l) are novel anthracyclines that have not been previously described, demonstrating the potential of this combinatorial biosynthetic method for the engineered generation of doxorubicin analogs with modified sugar moieties and the creation of improved anticancer agents.

Analysis of the metabolites produced by various combinations of genes encoding glycosylaransferases and sugar biosynthesis provided valuable information on their substrate flexibility and functions, although concurrent biochemical experiments were not carried out here. Introduction of the respective plasmids into *S. venezuelae* YJ183 did not cause any phenotypic difference, implying that expression plasmids did not affect the expression or activities of other host genes involved in growth, differentiation, and the production of other secondary metabolites. The glycosyltransferase AknS has been shown to accept aklavinone and ε-RHO as sugar acceptors and L-rhodosamine, L-rhamnose, L-daunosamine, and 2-deoxy-L-fucose as sugar donors (18, 21). Production of structurally diverse rhodomycin D derivatives in the present study showed that AknS has relaxed substrate specificity toward various L-aminosugars and L- and D-neutral sugars. The flexibility of the glycosyltransferase StfG in recognizing seven neutral sugars with different degrees of deoxygenation has been established in other work (30). Generation of 4′-*epi*-rhodomycin D (compound 1b) indicated that ε-RHO and 4-*epi*-L-daunosamine could be recognized and accepted by StfG. The glycosyltransferase SnogE showed the highest amino acid identity (59%) when the amino acid sequences of the glycosyltransferases SnogE, SnogD, and SnogZ present in the nogalamycin biosynthetic gene cluster from *S. nogalager* (42) were compared to that of AknS. The sequence comparison suggests that SnogE might transfer TDP-L-nogalose at the C-7 hydroxyl group of nogalamycin aglycone, and the production of 4′-*epi*-rhodomycin D by SnogE also supports this hypothesis. In addition, the auxiliary protein SnogN, which is essential for the glycosyl transfer activity of SnogE, was found. When the pEDNS4 derivative lacking *snogN* was expressed in YJ183, 4′-*epi*-rhodomycin D (compound 1b) was not detected (data not shown). Many previous studies have reported that the glycosyltransferase/auxiliary protein pair is necessary for the efficient transfer of deoxysugar in the biosynthesis of macrolide and anthracycline compounds (11, 21, 50), and the gene encoding the auxiliary protein was generally located immediately upstream of the glycosyltransferase gene in anthracycline and macrolide biosynthetic gene clusters. However, *snogN* has been found to be located 7 kb away from *snogE*, making it an unusual arrangement of genes.

The formation of 4′-*epi*-rhodomycin D (compound 1b), L-ristosaminyl-rhodomycin D (compound 1c), or both during the test of TDP-4-ketohexose reductases is an interesting outcome of the present study. It can be explained through DnmU being able to act not only as a 3,5-epimerase (in the formation of 4′-*epi*-rhodomycin D [compound 1b]) but also as a 5-epimerase (in the formation of L-ristosaminyl-rhodomycin D [compound 1c)] to cause an equilibrium of C-3,C-5 and C-5 epimers of TDP-3-amino-2,3,6-trideoxy-4-keto-D-glucose, one of them being a better substrate for each of the TDP-4-ketohexose reductases tested (Fig. 1B). It has been shown that GDP-mannose-3′,5′-epimerase (GME), an enzyme involved in the conversion of GDP-D-mannose to GDP-L-galactose, catalyzes two different epimerization reactions resulting in the production of two discrete products: GDP-L-glucose (by 5-epimerization) and GDP-L-galactose (by 3,5-epimerization). (47). These two distinct epimerization reactions of GME support the hypothesis that DnmU could catalyze both 3,5 and 5 epimerizations, producing TDP-4-keto-L-daunosamine and TDP-4-keto-L-ristosamine, respectively. Production of 4′-*epi*-rhodomycin D (1b) and L-ristosaminyl-rhodomycin D (compound 1c) by YJ183 mutants harboring pEDNS1 and its derivatives (pEDNS5, pEDNS6, pRST1, pRST2, pRST3, pRST4, and pRST5) indicates that the TDP-4-ketohexose reductases examined could accept 4-keto-L-daunosamine, 4-keto-L-ristosamine, or both as substrates. AvrE, which supported the highest epirubicin production, accepted TDP-4-keto-L-daunosamine (the C-3,C-5 epimer of TDP-3-amino-2,3,6-trideoxy-4-keto-D-glucose) as a glycosyl donor more efficiently than it did TDP-4-keto-L-ristosamine (the C-5 epimer of TDP-3-amino-2,3,6-trideoxy-4-keto-D-glucose). GrsB, which is involved in the biosynthesis of streptomycin, was also capable of reducing TDP-4-keto-L-daunosamine to produce TDP-4-*epi*-L-daunosamine. JadV, OleU, TylCIV, StrL, and SnogC, which participate in the biosynthesis of jadomycin B, oleandomycin, tylosin, streptomycin, and nogalamycin, respectively, were able to reduce TDP-4-keto-L-ristosamine mostly. EvaE, which encodes a TDP-4-ketohexose reductase involved in the biosynthesis of chloroeremomycin, can act on both intermediates generating both TDP-4-*epi*-L-daunosamine and TDP-L-ristosamine.

Production of 4′-*epi*-rhodomycin D (compound 1b) and L-ristosaminyl-rhodomycin D (compound 1c) in YJ183/pEVCS showed relaxed substrate specificity of both 5-epimerase EvaD

and 4-ketoreductase EvaE from the 4-*epi*-L-vancosamine biosynthetic pathway. It has previously been reported that 5-epimerase EvaD can accept TDP-3-amino-2,3,6-trideoxy-3-methyl-4-keto-D-glucose and epimerize at C-5 to produce TDP-4-keto-L-vancosamine, which is reduced at C-4 by 4-ketoreductase EvaE to generate TDP-4-*epi*-L-vancosamine (5). In addition, it had been demonstrated that EvaD also possesses the activity of 3,5-epimerase, catalyzing double epimerization of TDP-4-keto-6-deoxy-D-glucose at C-3 and C-5 (27). In the present study, 4′-*epi*-rhodomycin D (compound 1b), L-ristosaminyl-rhodomycin D (compound 1c), and 4′-*epi*-L-vancosaminyl-rhodomycin D (compound 1d) produced in YJ183/pEVCS indicated EvaD epimerizes both at C-5 and at C-3 and C-5 in TDP-3-amino-2,3,6-trideoxy-4-keto-D-glucose, and EvaE reduces both products of EvaD to synthesize both TDP-L-ristosamine and TDP-4-*epi*-L-daunosamine, which showed that EvaD and EvaE can recognize the unnatural substrates lacking a methyl group at C-3 in their natural substrates.

3′-*N*-Methyl-rhodomycin D (compound 1e), 3′-*N*-methyl-4′-*epi*-rhodomycin D (compound 1f), and 3′-*N*-methyl-L-ristosaminyl-rhodomycin D (compound 1g) were found from the cultures of YJ183 mutants expressing the plasmids pMDNS1, pMEDNS, and pMRST, respectively, which contain *aknX2* encoding *N*-methyltransferase from the biosynthetic pathway of TDP-L-rhodosamine (TDP-3-dimethyl-L-daunosamine). This showed that AknX2 was able to transfer a methyl group at the C-3 amine in TDP-L-daunosamine, TDP-4-*epi*-L-daunosamine, and TDP-L-ristosamine, indicating that AknX2 possesses the activity of *N*-methyltransferase and a certain relaxation of specificity. AknX2 had been thought to be a *N,N*-dimethyltransferase catalyzing the transfer of two methyl groups at the C-3 amine in TDP-L-daunosamine based on sequence comparison with other *N,N*-dimethyltransferases that have been experimentally characterized (38). However, YJ183 mutant carrying L-daunosamine biosynthetic genes and *aknX2* (YJ183/pMDNS1) produced significant amounts of 3′-*N*-methyl-rhodomycin D (compound 1e) and a trace amount of L-rhodosaminyl-rhodomycin D (compound 1h), suggesting that another *N*-methyltransferase might act on TDP-3-*N*-methyl-L-daunosamine for synthesizing TDP-L-rhodosamine. Interestingly, *S. galilaeus* 3AR-33 (25), an aklavinone-accumulating mutant derived from another aclacinomycin A producer, *S. galilaeus* ATCC 31133, has the aclacinomycin A biosynthetic gene cluster which has a similar genetic organization to that of *S. galilaeus* ATCC 31615 but harbors another *N*-methyltransferase gene, *aclP*, at a different location from that of *aknX2* in *S. galilaeus* ATCC 31615. When TDP-L-daunosamine biosynthesis genes and *aclP* were expressed in YJ183 (YJ183/pMDNS2), a large amount of 3′-*N*-methyl-rhodomycin D (compound 1e) and a trace amount of L-rhodosaminyl-rhodomycin D (compound 1h) were observed. YJ183 mutant containing the TDP-L-daunosamine-synthesizing gene cassette, *aknX2*, and *aclP* (YJ183/pRDS) produced significant amounts of 3′-*N*-methyl-rhodomycin D (compound 1e) and L-rhodosaminyl-rhodomycin D (compound 1h). Therefore, it is likely that two *N*-methyltransferases, AknX2 and AclP, are required for the efficient biosynthesis of TDP-L-rhodosamine.

ACKNOWLEDGMENTS

This study was supported by National Research Laboratory program 20100018430 through the Nation Research Foundation of Korea (NRF); NRF grants 2010K000890 and 20100001487 funded by the Ministry of Education, Science, and Technology; the National R&D Program for Cancer Control (grant 0620029); and the Marine and Extreme Genome Research Center Program of the Ministry of Land, Transportation and Maritime Affairs, Republic of Korea.

REFERENCES

1. **Acramone, F., et al.** 1997. New developments in antitumor anthracyclines. Pharmacol. Ther. **76:**117–124.
2. **Acramone, F., and G. Cassinelli.** 1998. Biosynthetic anthracyclines. Curr. Med. Chem. **5:**391–419.
3. **Bate, N., A. R. Butler, I. P. Smith, and E. Cundliffe.** 2000. The mycarose-biosynthetic genes of *Streptomyces fradiae*, producer of tylosin. Microbiology **146:**139–146.
4. **Bierman, M., et al.** 1992. Plasmid cloning vectors for the conjugal transfer of DNA from *Escherichia coli* to *Streptomyces* spp. Gene **116:**43–49.
5. **Chen, H., et al.** 2000. Deoxysugars in glycopeptide antibiotics: enzymatic synthesis of TDP-L-epivancosamine in chloroeremomycin biosynthesis. Proc. Natl. Acad. Sci. U. S. A. **97:**11942–11947.
6. **Essery, J. M., and T. W. Doyle.** 1980. The synthesis of daunosaminyl ε-rhodonycinone, daunosaminyl 10-*epi*-ε-rhodomycinone, daunosaminyl ε-pyrromycinone, and 10-descarbomethoxy-ε-pyrromycin. Can. J. Chem. **58:**1869–1874.
7. **Fan, E., W. Shi, and T. L. Lowary.** 2007. Synthesis of daunorubicin analogues containing truncated aromatic cores and unnatural monosaccharide residues. J. Org. Chem. **72:**2917–2928.
8. **Fischer, C., et al.** 2002. Digitoxosyltetracenomycin C and glucosyltetracenomycin C, two novel elloramycin analogues obtained by exploring the sugar donor substrate specificity of glycosyltransferase ElmGT. J. Nat. Prod. **65:**1685–1689.
9. **Guilfoile, P. G., and C. R. Hutchinson.** 1991. A bacterial analog of the *mdr* gene of mammalian tumor cells is present in *Streptomyces peucetius*, the producer of daunorubicin and doxorubicin. Proc. Natl. Acad. Sci. U. S. A. **88:**8553–8557.
10. **Hong, J. S. J., S. H. Park, C. Y. Choi, J. K. Sohng, and Y. J. Yoon.** 2004. New olivosyl derivatives of methymycin/pikromycin from an engineered strain of *Streptomyces venezuelae*. FEMS Microbiol. Lett. **238:**291–299.
11. **Hong, J. S. J., et al.** 2007. Functional analysis of *desVIII* homologues involved in glycosylation of macrolide antibiotics by interspecies complementation. Gene **386:**123–130.
12. **Hurteloup, P., and F. Ganzina.** 1986. Clinical studies with new anthracyclines: epirubicin, idarubicin, esorubicin. Drugs Exp. Clin. Res. **12:**233–246.
13. **Jung, W. S., et al.** 2006. Heterologous expression of tylosin polyketide synthase and production of a hybrid macrolide in *Streptomyces venezuelae*. Appl. Microbiol. Biotechnol. **72:**763–769.
14. **Jung, W. S., et al.** 2007. Bioconversion of 12-, 14-, and 16-membered ring aglycones to glycosylated macrolides in an engineered strain of *Streptomyces venezuelae*. Appl. Microbiol. Biotechnol. **76:**1373–1381.
15. **Jung, W. S., et al.** 2008. Enhanced heterologous production of desosaminyl macrolides and their hydroxylated derivatives by overexpression of the *pikD* regulatory gene in *Streptomyces venezuelae*. Appl. Environ. Microbiol. **74:**1972–1979.
16. **Kieser, T., M. J. Bibb, M. J. Buttner, K. F. Chater, and D. A. Hopwood.** 2000. Practical *Streptomyces* genetics. John Innes Centre, Norwich, United Kingdom.
17. **Kim, B. S., S. S. Moon, and B. K. Hwang.** 2000. Structure elucidation and antifungal activity of an anthracycline antibiotic, daunomycin, isolated from *Actinomadura roseola*. J. Agric. Food Chem. **48:**1875–1881.
18. **Leimkuhler, C., et al.** 2007. Characterization of rhodosaminyl transfer by the AknS/AknT glycosylation complex and its use in reconstituting the biosynthetic pathway of aclacinomycin A. J. Am. Chem. Soc. **129:**10546–10550.
19. **Lomovskaya, N., et al.** 1996. The *Streptomyces peucetius drrC* gene encodes a UvrA-like protein involved in daunorubicin resistance and production. J. Bacteriol. **178:**3238–3245.
20. **Lomovskaya, N., et al.** 1999. Doxorubicin overproduction in *Streptomyces peucetius*: cloning and characterization of the *dnrU* ketoreductase and *dnrV* genes and the *doxA* cytochrome P-450 hydroxylase gene. J. Bacteriol. **181:**305–318.
21. **Lu, W., et al.** 2005. AknT is an activating protein for the glycosyltransferase AknS in L-aminodeoxysugar transfer to the aglycone of aclacinomycin A. Chem. Biol. **12:**527–534.
22. **Madduri, K., F. Torti, A. L. Colombo, and C. R. Hutchinson.** 1993. Cloning and sequencing of a gene encoding carminomycin 4-*O*-methyltransferase from *Streptomyces peucetius* and its expression in *Escherichia coli*. J. Bacteriol. **175:**3900–3904.
23. **Madduri, K., and C. R. Hutchinson.** 1995. Functional characterization and transcriptional analysis of a gene cluster governing early and late steps in daunorubicin biosynthesis in *Streptomyces peucetius*. J. Bacteriol. **177:**3879–3884.
24. **Madduri, K., et al.** 1998. Production of the antitumor drug epirubicin (4′-epidoxorubicin) and its precursor by a genetically engineered strain of *Streptomyces peucetius*. Nat. Biotechnol. **16:**69–74.

25. **Matsuzawa, Y., et al.** 1981. New anthracycline metabolites from mutant strains of *Streptomyces galilaeus* MA144-M1. II. Structure of 2-hydroxyaklavinone and new aklavinone glycosides. J. Antibiot. **34:**959–964.
26. **Mendlik, M. T., P. Tao, C. M. Hadad, R. S. Coleman, and T. L. Lowary.** 2006. Synthesis of L-daunosamine and L-ristosamine glycosides via photoinduced aziridination: conversion to thioglycosides for use in glycosylation reaction. J. Org. Chem. **71:**8059–8070.
27. **Merkel, A. B., et al.** 2004. The position of a key tyrosine in dTDP-4-keto-6-deoxy-D-glucose-5-epimerase (EvaD) alters the substrate profile for this RmlC-like enzyme. J. Biol. Chem. **279:**32684–32691.
28. **Minotti, G., P. Menna, E. Salvatorelli, G. Cairo, and L. Gianni.** 2004. Anthracyclines: molecular advances and pharmacologic developments in antitumor activity and cardiotoxicity. Pharmacol. Rev. **56:**185–229.
29. **Olano, C., N. Lomovskaya, L. Fonstein, J. T. Roll, and C. R. Hutchinson.** 1999. A two-plasmid system for the glycosylation of polyketide antibiotics: bioconversion of ε-rhodomycinone to rhodomycin D. Chem. Biol. **6:**845–855.
30. **Olano, C., et al.** 2008. Glycosylated derivatives of steffimycin: insights into the role of the sugar moieties for the biological activity. Chembiochem **9:**624–633.
31. **Olano, C., C. Méndez, and J. A. Salas.** 2009. Antitumor compounds from actinomycetes: from gene clusters to new derivatives by combinatorial biosynthesis. Nat. Prod. Rep. **26:**628–660.
32. **Otten, S. L., X. Liu, J. Ferguson, and C. R. Hutchinson.** 1995. Cloning and characterization of the *Streptomyces peucetius dnrQS* genes encoding a daunosamine biosynthesis enzyme and a glycosyl transferase involved in daunorubicin biosynthesis. J. Bacteriol. **177:**6688–6692.
33. **Park, J. W., et al.** 2008. Genetic dissection of the biosynthetic route to gentamicin A2 by heterologous expression of its minimal gene set. Proc. Natl. Acad. Sci. U. S. A. **105:**8399–8404.
34. **Park, S. R., et al.** 2008. Heterologous production of epothilones B and D in *Streptomyces venezuelae*. Appl. Microbiol. Biotechnol. **81:**109–117.
35. **Park, S. R., et al.** 2009. Engineering of plant-specific phenylpropanoids biosynthesis in *Streptomyces venezuelae*. J. Biotechnol. **141:**181–188.
36. **Pérez, M., et al.** 2006. Combinatorial biosynthesis of antitumor deoxysugar pathways in *Streptomyces griseus*: reconstitution of "unnatural natural gene clusters" for the biosynthesis of four 2,6-D-dideoxyhexoses. Appl. Environ. Microbiol. **72:**6644–6652.
37. **Pissowotzki, K., K. Mansouri, and W. Piepersberg.** 1991. Genetics of streptomycin production in *Streptomyces griseus*: molecular structure and putative function of genes *strELMB2N*. Mol. Gen. Genet. **231:**113–123.
38. **Räty, K., T. Kunnari, J. Hakala, P. Mäntsälä, and K. Ylihonko.** 2000. A gene cluster from *Streptomyces galilaeus* involved in glycosylation of aclarubicin. Mol. Gen. Genet. **264:**164–172.
39. **Rodráiguez, L., et al.** 2002. Engineering deoxysugar biosynthetic pathways from antibiotic-producing microorganisms. A tool to produce novel glycosylated bioactive compounds. Chem. Biol. **9:**721–729.
40. **Schmitt-John, T., and J. W. Engels.** 1992. Promoter constructions for efficient secretion expression in *Streptomyces lividans*. Appl. Microbiol. Biotechnol. **36:**493–498.
41. **Sibi, M. P., J. Lu, and J. Edwards.** 1997. A new route to 3-amino sugars: a concise synthesis of L-daunosamine and D-ristosamine derivatives. J. Org. Chem. **62:**5864–5872.
42. **Torkkell, S., et al.** 2001. The entire nogalamycin biosynthetic gene cluster of *Streptomyces nogalater*: characterization of a 20-kb DNA region and generation of hybrid structures. Mol. Genet. Genomics **266:**276–288.
43. **Volchegursky, Y., Z. Hu, L. Katz, and R. McDaniel.** 2000. Biosynthesis of the anti-parasitic agent megalomicin: transformation of erythromycin to megalomicin in *Saccharopolyspora erythraea*. Mol. Microbiol. **37:**752–762.
44. **Wang, L., R. L. White, and L. C. Vining.** 2002. Biosynthesis of the dideoxysugar component of jadomycin B: genes in the *jad* cluster of *Streptomyces venezuelae* ISP5230 for L-digitoxose assembly and transfer to the angucycline aglycone. Microbiology **148:**1091–1103.
45. **Weymouth-Wilson, A. C.** 1997. The role of carbohydrates in biologically active natural products. Nat. Prod. Rep. **14:**99–110.
46. **Wohlert, S., et al.** 2001. Insights about the biosynthesis of the avermectin deoxysugar L-oleandrose through heterologous expression of *Streptomyces avermitilis* deoxysugar genes in *Streptomyces lividans*. Chem. Biol. **8:**681–700.
47. **Wolucka, B. A., and M. Van Montagu.** 2003. GDP-mannose 3′,5′-epimerase forms GDP-L-gulose, a putative intermediate for the de novo biosynthesis of vitamin C in plants. J. Biol. Chem. **278:**47483–47490.
48. **Xue, Y., L. Zhao, H. W. Liu, and D. H. Sherman.** 1998. A gene cluster for macrolide antibiotic biosynthesis in *Streptomyces venezuelae*: architecture of metabolic diversity. Proc. Natl. Acad. Sci. U. S. A. **95:**12111–12116.
49. **Yoon, Y. J., et al.** 2002. Generation of multiple bioactive macrolides by hybrid modular polyketide synthases in *Streptomyces venezuelae*. Chem. Biol. **9:**203–214.
50. **Yuan, Y., et al.** 2005. In vitro reconstitution of EryCIII activity for the preparation of unnatural macrolides. J. Am. Chem. Soc. **127:**14128–14129.